CIRP Annals – Manufacturing Technology
Volume 68, Issue 1, 2019, Pages 185-188

Sink electrical discharge machining of hydrophobic surfaces

Changcheng Guo[1], Philip Koshy[1] (1), Felipe Coelho[2], P. Ravi Selvaganapathy[1]

[1] Department of Mechanical Engineering, McMaster University, Hamilton, Canada
[2] Department of Mechanical Engineering, Sao Paulo State University, Bauru, Brazil

Abstract: The phenomenon of hydrophobicity observed in such surfaces as lotus leaves is typically manifest by hierarchical structures on low-energy surfaces. Sustained interest in fabricating hydrophobic surfaces has resulted in a myriad of processes, which are but limited by their largely referring to soft materials and/or involving multiple process steps. The present work explored the application of electrical discharge machining (EDM) for the single-step manufacture of durable, metallic hydrophobic surfaces. Simple sink EDM in a hydrocarbon dielectric, with no special process kinematic or tooling requirements, is demonstrated to rapidly generate surfaces that are intrinsically water repellent, with contact angles approaching 150°.

Keywords: Material removal, texture, topography

1. Introduction

Among the many biomimetic phenomena, scientists and engineers have perhaps been the most inspired by the water repellent behaviour of organic surfaces, which has accordingly translated into intriguing applications like anti-biofouling and anti-icing. This has in turn spurred the development of a multitude of processes for the fabrication of hydrophobic surfaces, examples of which include electrospinning, sol-gel processing and lithography. Such processes commonly pertain to soft materials like polymers, which are unsuitable for applications that demand mechanical durability; it is as well an issue that most of these processes necessitate supplementary steps such as coating or etching to functionalize the fabricated surface [1]. In this context, generation of robust metallic hydrophobic surfaces by machining in a single step is of significant interest.

The literature on machining of water repellent surfaces refers predominantly to laser micromachining of a grid of fine micro-grooves to generate an array of micro-pillars and micro-cavities. Such surfaces are rendered hydrophobic over several weeks on exposure to air, which for some materials may be accelerated by secondary low temperature annealing [2]. Laser micromachining corresponds to poor productivity even otherwise, considering that the micro-grooves are required to be spaced apart at a pitch of ~100 μm or less.

There have been just a handful of papers on electrical discharge machining (EDM) of hydrophobic surfaces. Ref. [3] details micro-EDM of three-dimensional, mushroom-like structures in steel using a 20 μm diameter wire, using the kinematic shown in Fig. 1a, about two perpendicular planes. The process is rather intricate and machining time-intensive: the pitch between the re-entrant features is ~200 μm, and it takes ~60 s for each machining pass corresponding to a length of 10 mm. A maximum contact angle (CA) of 160° was obtained in this work, but the machined surface was dip-coated in Teflon, which in itself is hydrophobic.

Ref. [1] pertains to the application of conventional wire EDM in deionized water to generate 2.5-dimensional sinusoidal surfaces (Fig. 1b) of a wavelength in the range of 200–500 μm by programming the wire path, to yield a maximum water CA of 157°. This concept was later extended to wire EDM of rectangular microgrooves (Fig. 1c) of several hundred μm in size [4]. Owing to the nature of wire EDM, such approaches are intrinsically limited to fabricating swept surfaces that are anisotropic.

The method adopted in [5] entailed a sequence of steps (Fig. 1d), the first of which was EDM milling in a kerosene dielectric as a platform for creating a hydrophobic surface, which increased the water CA of copper from 66° to 95°. The surface was subsequently coated with carbon nanoparticles by exposing it to a butane flame, which enhanced the CA substantially to 168°. The carbon layer was however quite fragile, and had to be rendered robust by impregnating it with oil, followed by heat treatment. In the work reported in [6], micro-holes were laser-drilled in a copper foil, which was then used as the electrode to reverse micro-EDM a two-dimensional array of 50 μm diameter micro-pillars. This elaborate, two-step process corresponded to a maximum water CA of 115° in the Ti6Al4V alloy.

As seen above, the prior art on EDM of hydrophobic surfaces has entailed either specialized tooling, process kinematics, additional process steps or a combination thereof, which limits productivity. The work presented in this paper was hence embarked on to explore the viability of rapidly generating three-dimensional, durable, isotropic hydrophobic surfaces using simple, one-dimensional sink EDM in a single step, unencumbered by such tooling and kinematic requirements.

Such an unconventional application of sink EDM was inspired by the recognition that it is one of the few machining processes capable of generating three-dimensional surfaces with a positively-skewed height distribution (Fig. 2a). This denotes that the machined surface comprises few peaks interspersed among many valleys as shown schematically in Fig. 2b. This disposes it as a stochastic, composite solid-liquid-air interface, wherein the

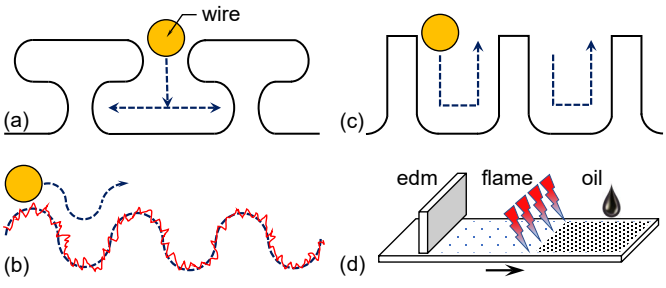

Fig. 1. Prior art on EDM of hydrophobic surfaces.

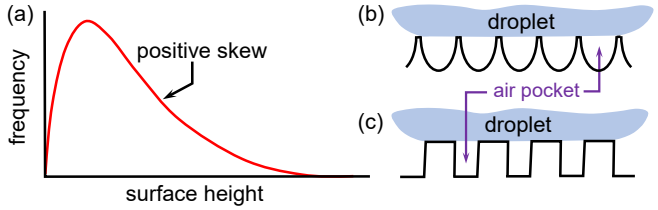

Fig. 2. Rationale for simple sink EDM of hydrophobic surfaces.

troughs constitute air pockets that can cushion a liquid droplet atop the peaks in the Cassie-Baxter state, in contrast to the Wenzel state wherein the liquid intrudes into the interstices to form a homogenous wetted interface [7]. Such a surface is similar to hydrophobic surfaces comprising micro-pillars (Fig. 2c), the fabrication of which is but significantly more involved. Given that such a texturing application refers to the removal of a rather thin layer of material, the relatively low removal rate of EDM is of little consequence, and the process can prove competitive to laser texturing in terms of machining time. Key EDM parameters viz. the discharge current and duration may further be varied to tailor the surface topography towards enhancing its functionality.

2. Experimental

With a view to exploring the feasibility of generating hydrophobic surfaces and comprehending the underlying mechanisms, sink EDM experiments were conducted on 7075 aluminum alloy using copper electrodes, over a range of discharge current i_e and discharge duration t_e at either polarity, largely using hydrocarbon oil as the dielectric fluid. The open circuit voltage and duty factor were kept constant at 100 V and 0.4, respectively. The machining gap was flushed using periodic electrode retraction. The tool surface was trued by fine milling before each experiment to preclude any confounding influence of the remnant tool roughness.

Surface wetting was characterized in terms of the static CA with deionized water as the probing liquid, measured using the sessile drop technique by dispensing 6 µL droplets. All machined surfaces were cleaned using a commercial solvent meant for electrical contacts, which was confirmed to not influence wetting by measuring the CA after rinsing the solvent off the surface. Measurements were completed 24 hours after machining, unless noted otherwise. CA was estimated using the ellipse fitting method, which was verified manually using image processing software to yield accurate values; the Young-Laplace method used in such works as [5] was found to overestimate the CA by as much as 15°, as cautioned in [7]. Six CA measurements (two each on three samples of 15×12 mm² area) were completed for each parameter combination to capture the variability. Machined surfaces were investigated using confocal and scanning electron microscopy; they were additionally subject to X-ray photoelectron spectroscopy (XPS) to characterize their surface chemistry.

3. Results and discussion

The first phase of this research focused on the effect of pulse parameters on the CA. Fig. 3a and 3b show the CA obtained using simple sink EDM (termed primary texturing) as a function of the discharge current for discharge durations of 6.5 µs and 18 µs, respectively. The CA increased quite significantly to more than twice that of the equilibrium (Young) CA of 59° corresponding to a flat polished surface, and exhibited a declining trend with an increase in discharge current. The observed variability in CA is typical of machined hydrophobic surfaces [3], and is indicative of the several metastable states referring to local energy minima that the water droplet can exist in. For over a twenty-fold variation in pulse energy corresponding to a roughness range of

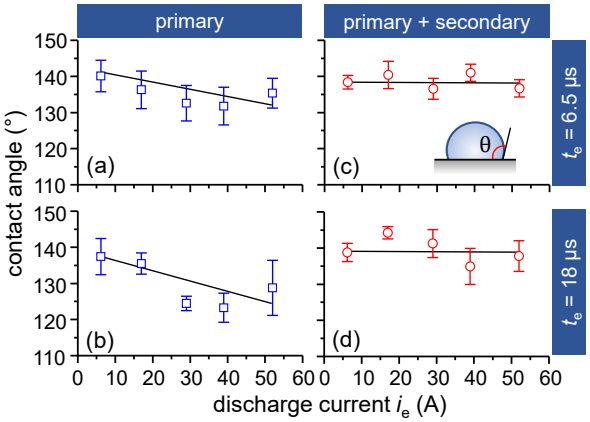

Fig. 3. Effect of i_e and secondary texturing on CA (θ).

1.4–8.0 µm *Ra*, the change in CA is in the range of just about 20°. This is consistent with the report in [1] on wire EDM of hydrophobic surfaces, wherein for a roughness range of 0.4–4.2 µm *Ra*, the CA was between 134° and 157°.

A biomimetic concept that has significantly enhanced the fabrication of hydrophobic surfaces is the notion of hierarchical structures. This idea has been inspired by organic surfaces like lotus leaves, which comprise paraboloidal protrusions that are 10–20 µm in size, on which sub-µm epicuticular wax crystalloids are situated. Free energy analysis and thermodynamic modelling have indicated such surfaces to relate to a higher water CA and lower hysteresis [7]. Given that factors that can destabilize the composite Cassie-Baxter state into the homogenous, lower-energy Wenzel state such as surface heterogeneities and capillary waves are scale-dependent, a dual-scale structure is better equipped to guard against such a transition [8].

Previous work on wire EDM of hydrophobic surfaces [1] has incorporated this knowledge by programming sinusoidal wire paths to generate first-order topographic features, on which the EDM craters were deemed to constitute second-order features (see Fig. 1b). The increment in CA from adopting such a dual-scale structure was however not quantified in [1]. The approach adopted in the present work is to generate a hierarchical structure by superimposing a finer texture over the primary texture (termed secondary texturing) by simply reducing the pulse energy significantly during the final several seconds of machining. Such an approach is elegant, free of any macro-geometric constraints on the machined surface and is readily executed under program control.

Fig. 3c and 3d show the corresponding changes to the CA from the addition of secondary texturing, relative to primary texturing alone (Fig. 3a and 3b), for the two discharge durations. Secondary texturing was applied for a duration of 5 s, and it referred to a discharge current and duration of 1.2 A and 0.4 µs, respectively, which were the lowest available on the machine tool. It is evident that the secondary texturing has rendered the CA to be essentially independent of the discharge current, and has reduced the variability in CA. This is significant in that the secondary texturing allows for both higher productivity and quality, given that the primary texturing may be accomplished at a higher discharge energy without conceding wetting resistance.

In order to understand the increase in CA and the decrease in its variability brought forth by secondary texturing, surfaces were examined using confocal microscopy. Fig. 4a shows a surface profile relating to just primary texturing (i_e 17 A, t_e 18 µs), and Fig. 4b a profile generated by both primary and secondary texturing. A comparison of these indicates the secondary texturing to have targeted and removed the high points on the surface from the primary texturing, rendering the profile height to be more uniform. Such selective pruning is logical given that discharges in EDM generally occur between closest points across the spark gap.

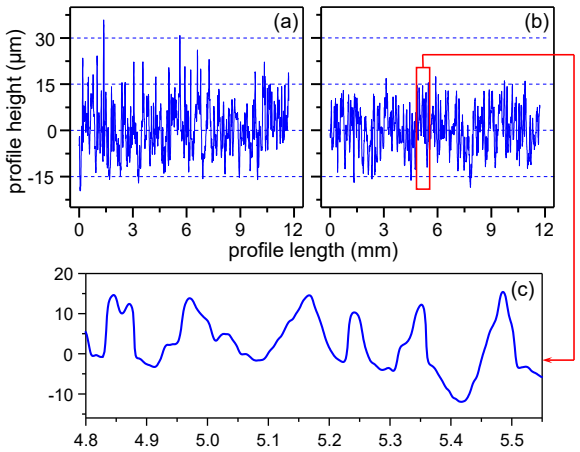

Fig. 4. Influence of secondary texturing on profile height.

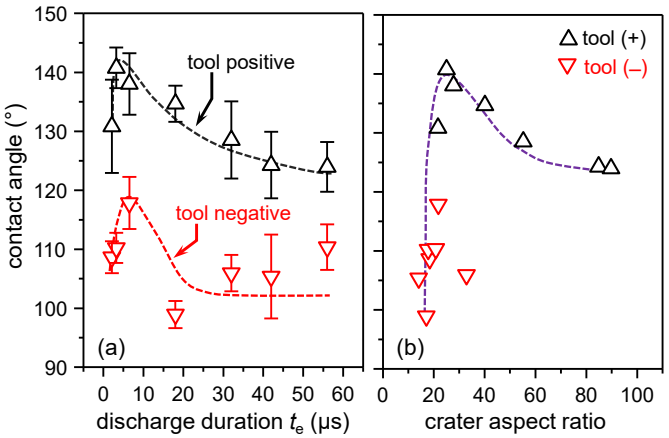

Fig. 6. Effect of polarity, t_e and crater shape on CA.

After secondary texturing, the profile was further seen to comprise convex features (Fig. 4c) with a peak to valley height of 10–20 μm in this instance, which incidentally is on the same order as that of the primary protruding features on lotus leaves [8].

To complement the analysis above, surfaces were also examined in a scanning electron microscope. Fig. 5 shows representative single- and dual-scale surfaces at two magnifications (areas demarcated by yellow rectangles in the left panel are shown magnified in the right). The surface subject to primary texturing alone (i_e 29 A, t_e 18 μs) seen in Fig. 5a and 5b shows characteristic EDM craters, with several hierarchical features on the surrounding rims. This offers an indication of how water droplets may be maintained in the Cassie-Baxter state, superficially on the elevated rim features around the crater periphery, supported by the volume of air trapped in the concave crater body beneath, as originally intended (Fig. 2b). The surface subject to both primary and secondary texturing (Fig. 5c and 5d) can be clearly seen to comprise additional fine secondary features that are relatively more pronounced (which were not adequately resolved during profilometry, Fig. 4b), localised on the crater rims (highlighted in Fig. 5d) that represent high points. Such secondary features tend to pin the contact line and help augment the CA [8].

Having grasped the role of secondary texturing, results shown hereinafter refer to primary texturing alone. In contrast to the discharge current that referred to a monotonic change in CA (Fig. 3a and 3b), the discharge duration indicated a non-linear response exhibiting maxima for both polarities (Fig. 6a). The CA for the tool-positive polarity was higher for all discharge durations investigated. Not unexpectedly, the CA revealed no correlation with roughness parameters like *Ra* and *Rz*. Considering that EDM surfaces are generated by repeated, random superposition

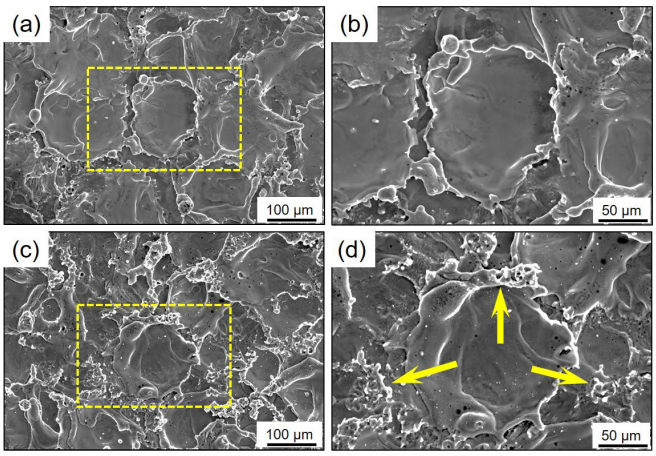

Fig. 5. Scanning electron micrographs of textured surfaces.

of numerous discharges, a characteristic crater geometry may be obtained by modelling the surface profile in the form of a first-order stochastic differential equation using the Data Dependent Systems methodology [9]. Fig. 6b elegantly consolidates the role of discharge duration and polarity in terms of the diameter to depth ratio of characteristic craters obtained thus from the corresponding surface profiles, which reveals the CA to be maximized in a rather narrow range of crater aspect ratio. It may be noted that a study on the effect of the geometry of deterministic micropillar array patterns on CA reports a similar trend in terms of the pillar pitch and height [8].

With the objective of exploring possible influences of factors other than surface topography reported thus far in this paper, experiments were also conducted using deionized water as the dielectric fluid (i_e 29 A, t_e 18 μs), and the time evolution of CA was tracked. This yielded intriguing results (Fig. 7). In stark contrast to the surface machined in oil, the surface generated in water was in fact initially hydrophilic; adding to the intrigue, the CA exhibited an increase in excess of 100° over the next 15 days on exposure to the ambient and levelled off thereafter. The surface machined in oil exhibited a relatively modest increase of ~10° over this period. A review of the pertinent literature returned Ref. [10] that reports a similar temporal evolution of CA for laser micromachined Al surfaces, which attributes it to the adsorption of organic species from the atmosphere. This hypothesis was verified in the present work by machining a sample in deionized water and leaving it immersed in water post-machining, which did not show any increase in CA (see Fig. 7), and in fact continued to exhibit complete surface wetting.

Relevant machined samples were therefore probed using XPS to examine their surface chemistry. Survey spectra indicated the presence of C and O, in addition to Zn, Cu, Mg, and Al that are to be expected for Al 7075. The level of C was the factor differentiating the surfaces investigated. Fig. 8 shows the ratio of atomic C to atomic Al that is a measure of the relative extent of the adsorbed organic compounds, which correlates with the CA, as established in [10]. The C/Al ratio is noticeably higher for surfaces

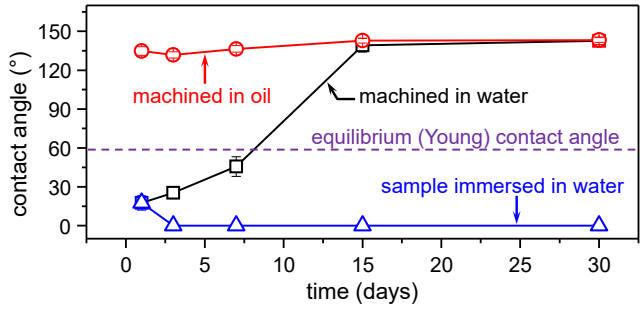

Fig. 7. Temporal evolution of CA for EDM in oil and water.

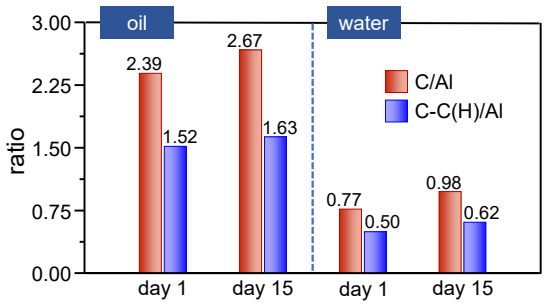

Fig. 8. Comparison C/Al and C-C(H)/Al ratios.

machined in oil, indicating better adsorption of organic compounds from solution (oil) than from gas-phase organics. This in part also explains the significant difference in CA between surfaces machined in oil and water, a day after machining; the C/Al ratio further increases from day 1 to day 15 for surfaces machined both in oil and water, which as well correlates with the temporal trends in the corresponding CA (Fig. 7).

To gain additional insights, the feature-rich C 1s peaks in the XPS spectra were deconvoluted to identify the functional groups in which C is present on EDM-textured surfaces. This revealed a main peak around a binding energy of 284.6 eV, indicative of the C–C(H) bond representing hydrocarbon chains that is (non-polar) hydrophobic, which is not easily removed by solvents [10]. The ratio of C–C(H) to Al depicted in Fig. 8 therefore further illuminates the CA trends in Fig. 7: the percentage change in this ratio over 15 days after machining is significantly higher for water (24%) as compared to oil (7%), which elucidates the respective evolution of their CA over this time.

It therefore follows that the CA on day 1 for surfaces machined in oil and water respectively being significantly higher and lower than the equilibrium CA referring to a smooth surface (Fig. 7) originates from the synergistic interplay between surface topography and surface chemistry. The surface machined in water is initially covered by a thin film of amorphous, hydrophilic aluminum oxide; the roughness induced by EDM texturing amplifies the hydrophilicity [7, 8]. Conversely, the surface machined in oil develops hydrophobicity due to the surface C adsorbed therefrom, which is further accentuated by the EDM texture.

In closing this section, Fig. 9 presents a visual proof-of-concept for sink EDM of hydrophobic surfaces. While water droplets deposited on a polished surface take on a pancake shape (Fig. 9a) with a CA of just 59° (Fig. 9b), those on one of the best surfaces textured by sink EDM can be seen to assume near-spherical shapes (Fig. 9c), with a CA of 149° (Fig. 9d), which is at the cusp of the threshold (150°) for superhydrophobicity. Such surfaces referred to a CA hysteresis in the range of 10° to 15°. High-speed imaging revealed these surfaces to be likewise starkly

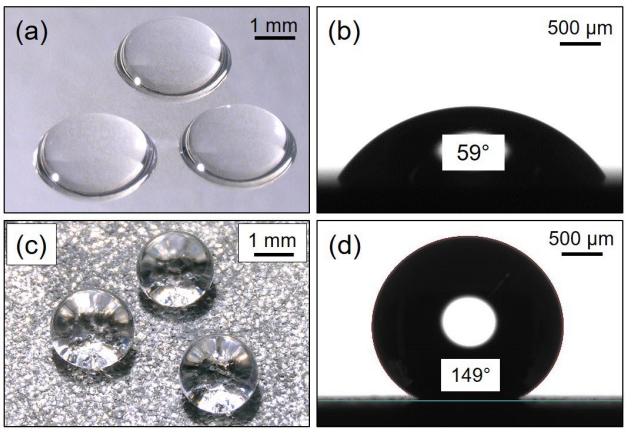

Fig. 9. A comparison of droplet shape and CA.

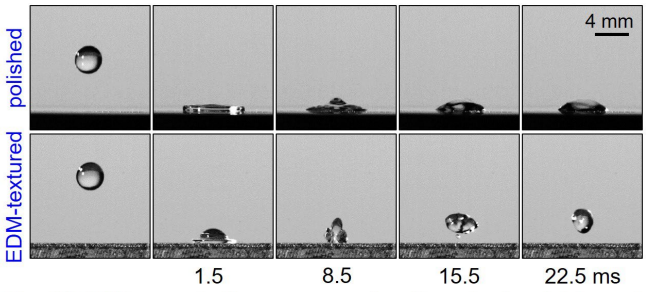

Fig. 10. Difference in the response of surfaces to droplet impact.

different with respect to their response to droplet impact (Fig. 10). While the impinging droplet (1 m/s impact velocity) stuck to and wetted the polished surface entirely, it manifested a complete rebound off the EDM-textured surface, signifying its hydrophobicity. It is remarkable that such water repellent surfaces of 15×12 mm^2 area can be textured using sink EDM in less than 2 minutes.

4. Conclusions

This research demonstrated a novel, unconventional application of simple sink EDM for fabricating robust, isotropic hydrophobic surfaces in aluminum, with no need for special tooling or process kinematics. The effect of pulse parameters and the dielectric medium on CA was investigated, and the wetting mechanism was clarified in terms of surface topography and surface chemistry. The proof-of-concept highlights the significant potential of oil-based sink EDM for the rapid fabrication of three-dimensional hydrophobic surfaces in a single step, and its scope for scale-up towards interesting applications in industry.

Acknowledgements

This work was funded by the Natural Sciences and Engineering Research Council of Canada through the Canadian Network for Research and Innovation in Machining Technology, and Pratt & Whitney Canada. PRS acknowledges support from the Canada Research Chairs Program.

References

[1] Bae WB et al. (2012) One-Step Process for Superhydrophobic Metallic Surfaces by Wire Electrical Discharge Machining. *Applied Materials & Interfaces* 4:3685–3691.

[2] Chun DM, Ngo CV, Lee KM (2016) Fast Fabrication of Superhydrophobic Metallic Surface Using Nanosecond Laser Texturing and Low-Temperature Annealing. *CIRP Annals–Manufacturing Technology* 65:519–522.

[3] Weisensee P et al. (2014) Hydrophobic and Oleophobic Re-Entrant Steel Microstructures Fabricated Using Micro Electrical Discharge Machining. *Journal of Micromechanics and Microengineering* 24:095020 (10 pp).

[4] Bae WB et al. (2015) Engineering Stainless Steel Surface via Electrical Discharge Machining for Controlling the Wettability. *Surface & Coatings Technology* 275:316–323.

[5] Dong S et al. (2018) Roll-to-Roll Manufacturing of Robust Superhydrophobic Coating on Metallic Engineering Materials. *Applied Materials & Interfaces* 10:2174–2184.

[6] Mastud S et al. (2012) Experimental Characterization of Vibration-Assisted Reverse Micro-Electrical Discharge Machining for Surface Texturing. *ASME Int. Manuf. Science & Eng. Conference*, Notre Dame, 1–10.

[7] Law KY, Zhao H (2016) *Surface Wetting*. Springer International Publishing, Switzerland.

[8] Bhushan B, Jung YC (2011) Natural and Biomimetic Artificial Surfaces for Superhydrophobicity, Self-Cleaning, Low Adhesion, and Drag Reduction. *Progress in Materials Science* 56:1–108.

[9] Pandit SM, Rajurkar KP (1980) Crater Geometry and Volume from Electro-Discharge Machined Surface by Data Dependent Systems. *Journal of Engineering for Industry* 102:289–295.

[10] Long J, Zhong M, Zhang H, Fan P (2015) Superhydrophilicity to Superhydrophobicity Transitions of Picosecond Laser Microstructured Aluminum in Ambient Air. *Journal of Colloid and Interface Science* 441:1–9.